









# Effect of H<sub>2</sub>S on the Near-infrared Spectrum of Irradiation Residue and Applications to the Kuiper Belt Object (486958) Arrokoth

Ahmed Mahjoub<sup>1,2</sup> , Michael E. Brown<sup>3</sup> , Michael J. Poston<sup>1,4</sup> , Robert Hodyss<sup>1</sup>, Bethany L. Ehlmann<sup>1,3</sup> , Jordana Blacksberg<sup>1</sup>, Mathieu Choukroun<sup>1</sup> , John M. Eiler<sup>3</sup>, and Kevin P. Hand<sup>1</sup> 

<sup>1</sup>Jet Propulsion Laboratory, California Institute of Technology, Pasadena, CA, USA

<sup>2</sup>Space Science Institute, 4765 Walnut Street, Suite B, Boulder, CO 80301, USA

<sup>3</sup>Division of Geological & Planetary Sciences, California Institute of Technology, Pasadena, 91125, USA

<sup>4</sup>Southwest Research Institute, San Antonio, TX, USA

Received 2021 April 15; revised 2021 May 11; accepted 2021 May 21; published 2021 June 17

## Abstract

On 2019 January 1, the New Horizons spacecraft flew by (486958) Arrokoth, a small body in the Kuiper Belt that is the most distant object ever visited by a spacecraft. A strong unidentified absorption band was observed in the spectrum of Arrokoth at 1.8  $\mu\text{m}$ . We report here experimental evidence suggesting that the near-infrared spectrum of Arrokoth is indicative of sulfur-rich, tholin-like organic residue. The spectra of organic residues produced by irradiating ice mixtures “with H<sub>2</sub>S” CH<sub>3</sub>OH:NH<sub>3</sub>:H<sub>2</sub>S:H<sub>2</sub>O (3:3:3:1) and “without H<sub>2</sub>S” CH<sub>3</sub>OH:NH<sub>3</sub>:H<sub>2</sub>O (3:3:1) were measured to study the effect of H<sub>2</sub>S. The “with H<sub>2</sub>S” sulfur-rich laboratory-synthesized organic residue displays an absorption band at 1.8  $\mu\text{m}$  that is absent in the spectrum of “without H<sub>2</sub>S” sample. This feature matches the Arrokoth spectrum better than any other expected material. This suggests the past presence of H<sub>2</sub>S ice on the surface of Arrokoth and a role for Kuiper Belt objects as a key S reservoir in the early solar system.

*Unified Astronomy Thesaurus concepts:* [Astrochemistry \(75\)](#); [Solar system \(1528\)](#); [Small Solar System bodies \(1469\)](#); [Laboratory astrophysics \(2004\)](#); [Trans-Neptunian objects \(1705\)](#); [Kuiper belt \(893\)](#)

## 1. Introduction

The Kuiper Belt contains primordial icy bodies believed to be remnants from the reservoir of planetesimals that surrounded the early solar system. The composition of these Kuiper Belt objects (KBOs), resulting from their starting chemistry and their history of surface processing, can be read and deciphered to gain more insight into the formation and evolution of the solar system. Growing evidence suggests that H<sub>2</sub>S was a highly abundant molecule in the presolar nebula. Recently, the Rosetta mission to comet Churyumov–Gerasimenko demonstrated that H<sub>2</sub>S is the fifth most abundant molecule in the coma after H<sub>2</sub>O, CO, CO<sub>2</sub>, and O<sub>2</sub> (Rubin et al. 2019). One important question is the effect of H<sub>2</sub>S on the composition and spectroscopy of organic residues, called tholins, that are believed to exist on the surfaces of small icy bodies, including KBOs (Cruikshank et al. 2005). Despite the importance of H<sub>2</sub>S and the potential of sulfur chemistry to considerably affect the chemical reactivity on the surfaces of airless bodies, little has been published exploring this chemistry. Also, H<sub>2</sub>S residues have not been directly detected on solar system bodies to date, although a recent study has shown evidence for sulfur-bearing species on Callisto’s leading hemisphere (Cartwright et al. 2020). We recently studied the role that H<sub>2</sub>S could play in the chemistry (Mahjoub et al. 2016, 2017), spectroscopy (Poston et al. 2018), and astrobiology (Mahjoub & Hodyss 2018) of small icy bodies—particularly KBOs and Jupiter Trojans (Wong et al. 2019)—and apply these results to Arrokoth.

Arrokoth is a member of the cold classical Kuiper Belt (CC-KBO), a collection of small bodies believed to have formed beyond the orbit of Neptune and to have never experienced large-scale change of orbit. Recent New Horizons spacecraft data show widespread abundant CH<sub>3</sub>OH, a reddish darkening agent(s) inferred to be a mixture of amorphous carbon and tholins, low abundances of water and ammonia, and a strong

1.8  $\mu\text{m}$  absorption, to date unexplained (Stern et al. 2019; Grundy et al. 2020). This absorption feature appears as strong as the other features identified in Grundy et al. (2020). The band was discussed previously but was not assigned to a molecular identification.

Here, we present spectra of organic residues produced with and without H<sub>2</sub>S to infer the effect of sulfur chemistry in the near-infrared (NIR) spectral region. We analyze the New Horizons data in concert with results from our laboratory experiments and show that S-bearing refractory organics derived from the products of irradiation of H<sub>2</sub>S on the surfaces of KBOs are a plausible source of the 1.8  $\mu\text{m}$  feature. We also discuss implication for reservoirs of S in the early solar system.

## 2. Experimental Methodology

Two residue samples were produced by irradiation of ice films under vacuum at 50 K. A tholin film “without sulfur” was produced from a starting ice of CH<sub>3</sub>OH:NH<sub>3</sub>:H<sub>2</sub>O (3:3:1), and a tholin film “with sulfur” was produced from a starting ice mixture of CH<sub>3</sub>OH:NH<sub>3</sub>:H<sub>2</sub>S:H<sub>2</sub>O (3:3:3:1). These samples are similar to our previous studies investigating spectroscopic and chemical properties of H<sub>2</sub>S containing ices (Mahjoub et al. 2016, 2017; Poston et al. 2018). Electron irradiation experiments were carried out using the Icy Worlds Simulation laboratory. A detailed description of the facilities and the capabilities of this laboratory can be found in Hand & Carlson (2011). The experimental setup consists of a high-vacuum stainless steel chamber pumped by a Varian Turbo pump and backed by oil-free pumps (pressure after overnight pumping about  $1 \times 10^{-8}$  torr). The ices were vapor-deposited on a substrate attached to the cold finger of a closed-cycle helium cryostat (ARS model DE-204). An external manifold was used to prepare gas mixtures prior to deposition. The ice films were

grown by leaking the gas mixture into the chamber and forming ices on the substrate, which was held at 50 K.

High-energy electrons (10 keV) were directed at the ice with a typical beam current of  $0.5 \mu\text{A}$ . All studied ices were submitted to the same fluence of electron energy  $\sim 2 \times 10^{21} \text{ eV cm}^{-2}$ . Radiation fluences were scaled to the outer solar system based on the electron flux at 1 au, which was deduced from values given in Bennett et al. (2013). We found that the total fluence received by our ice samples corresponds to a timescale of 0.2 Myr for an object at 5 au and 1.8 Myr at 15 au.

As discussed in Mahjoub et al. (2016), the chemical composition of ice films calculated using infrared spectra and band strengths of deposited molecules is different from the gas phase mixture. The compositions of the ices solid films as estimated from the respective column densities are:  $\text{CH}_3\text{OH-NH}_3\text{-H}_2\text{O} = 73:12:15$  for the “without  $\text{H}_2\text{S}$ ” ice and  $\text{H}_2\text{S-CH}_3\text{OH-NH}_3\text{-H}_2\text{O} = 7:35:17:41$  for the “with  $\text{H}_2\text{S}$ ” sample. After irradiation for 19 hr at 50 K, samples were warmed to 120 K at  $0.5 \text{ K minute}^{-1}$  rate and held there for 1 additional hour under continued electron irradiation. After the electron irradiation was concluded, the samples were warmed at  $0.5 \text{ K minute}^{-1}$  rate to 300 K. The resulting residue films were characterized at room temperature by specular reflectance spectroscopy, using a Midac FTIR spectrometer. The residue samples in both experiments were very thin films on top of a gold mirror, which made it difficult to characterize their colors. The “with  $\text{H}_2\text{S}$ ” residue appeared darker than the “without  $\text{H}_2\text{S}$ ” residue. A network of cracks appeared on the “without  $\text{H}_2\text{S}$ ” sample, while less-pronounced cracks were visible on the “with  $\text{H}_2\text{S}$ ” sample.

### 3. Results and Discussion

Figure 1 shows a comparison between the spectrum of the “without sulfur” and “with sulfur” residues. The spectrum of “without sulfur” residue is flat in the  $1.8 \mu\text{m}$  region, which agrees with spectra reported in the literature of CNOH-based tholins (Materese et al. 2015) and routinely used to model spectra of small icy bodies, including Arrokoth (Grundy et al. 2020). The spectrum of the “with sulfur” residue shows a pronounced band at  $1.8 \mu\text{m}$ . The depth of this band is approximately 2% of the baseline and the width at half maximum is around 100 nm. The sulfur-bearing residue is a complex chemical material, composed of a plethora of molecular species of CNOHS; therefore, the definitive assignment of this absorption band to a particular species is not currently possible. Nevertheless, because it only occurs in the  $\text{H}_2\text{S}$ -bearing ice mixture, this absorption could be tentatively assigned to a combination of  $\nu(\text{SH}) + \nu(\text{CH})$  in a family of molecules/functional groups rich in  $\text{C}_x\text{S}_y\text{H}_z$  moieties. This band could also be due to a combination between the  $\text{C}=\text{O}$  stretching modes in  $-\text{OCS}-$  groups at  $2050 \text{ cm}^{-1}$  and the  $\text{S}=\text{O}$  stretching mode around  $1400 \text{ cm}^{-1}$ :  $\nu(\text{SO}) + 2\nu(\text{CO})$ . A better characterization of the chemical composition of the residue, and isotope labeling tests, are needed to better constrain the sulfurous compounds or family of compounds responsible for this band. Such in-depth characterization of the sulfur-bearing residue is beyond of the scope of this Letter and will be investigated in future studies. Future studies will also investigate the evolution of the observed  $1.8 \mu\text{m}$  band as a function of thermal processing of the sample between 50 and 300 K. Spectra in the mid-infrared (MIR) show only limited

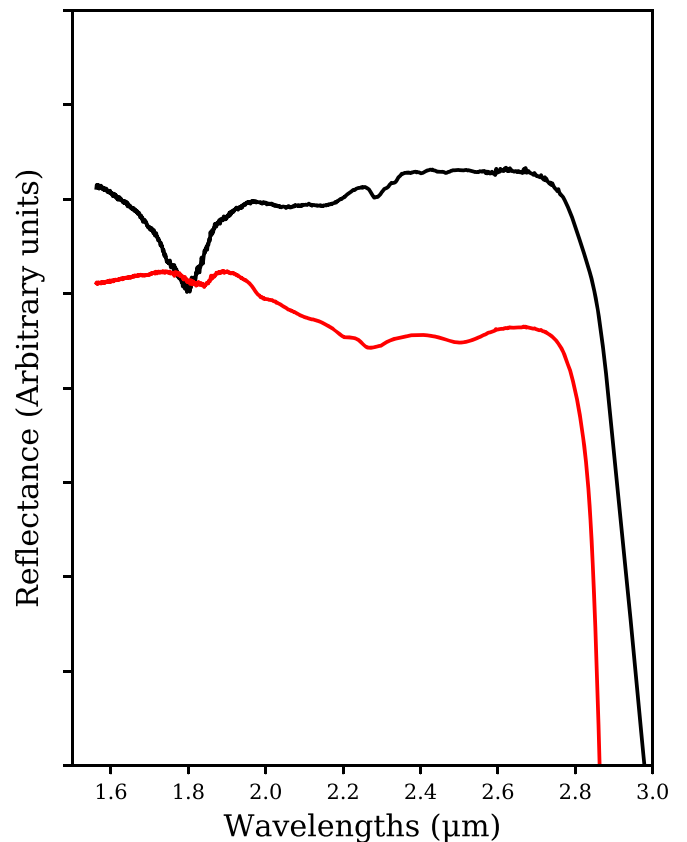


**Figure 1.** Comparison between spectra of the “without sulfur” (red) and “with sulfur” (black) residues produced by irradiation of ices  $\text{CH}_3\text{OH:NH}_3:\text{H}_2\text{O}$  (3:3:1) and  $\text{CH}_3\text{OH:NH}_3:\text{H}_2\text{S}:\text{H}_2\text{O}$  (3:3:3:1), respectively.

chemical evolution of the sample between 50 and 150 K (Mahjoub et al. 2016).

Figure 2 shows a comparison between the spectrum of Arrokoth and the spectrum of “with sulfur” residue. A good match between the two spectra at the band  $1.8 \mu\text{m}$  can be visually noted. We fit a linear mixture model including the spectra of methanol, “with sulfur” residue and “without sulfur” residue (Figure 2). Methanol and “without sulfur” residue spectra were added because in Grundy et al. (2020) the best fit was obtained using a model incorporating methanol and tholin. The model in Grundy et al. (2020) fit quite well the spectrum of Arrokoth except for the  $1.8 \mu\text{m}$  band. Adding the spectrum of “with sulfur” residue improves considerably the fit, especially the  $1.8 \mu\text{m}$  feature (Figure 2). This results in a very small residual difference between the spectrum of Arrokoth and the model, which is flat around  $1.8 \mu\text{m}$  confirming the good spectral alignment between the bands. Adding the “without sulfur” residue to the linear regression model improves the fit of the baseline of the spectrum but obviously is not able to reproduce the  $1.8 \mu\text{m}$  band. We cannot exclude the co-existence of both “with sulfur” and “without sulfur” on the surface of Arrokoth. We can speculate that, because  $\text{H}_2\text{S}$  is much faster consumed by irradiation chemistry than methanol, both “with sulfur” and “without sulfur” organics could be formed on the surface of the KBO. It is important to clarify that the model presented here cannot be used to determine the relative abundances of each of the compounds. The model-fitting coefficient is given in the Figure 2 caption. A more sophisticated model will need the refractive index of “with sulfur” residue, a measurement that is not available to date.

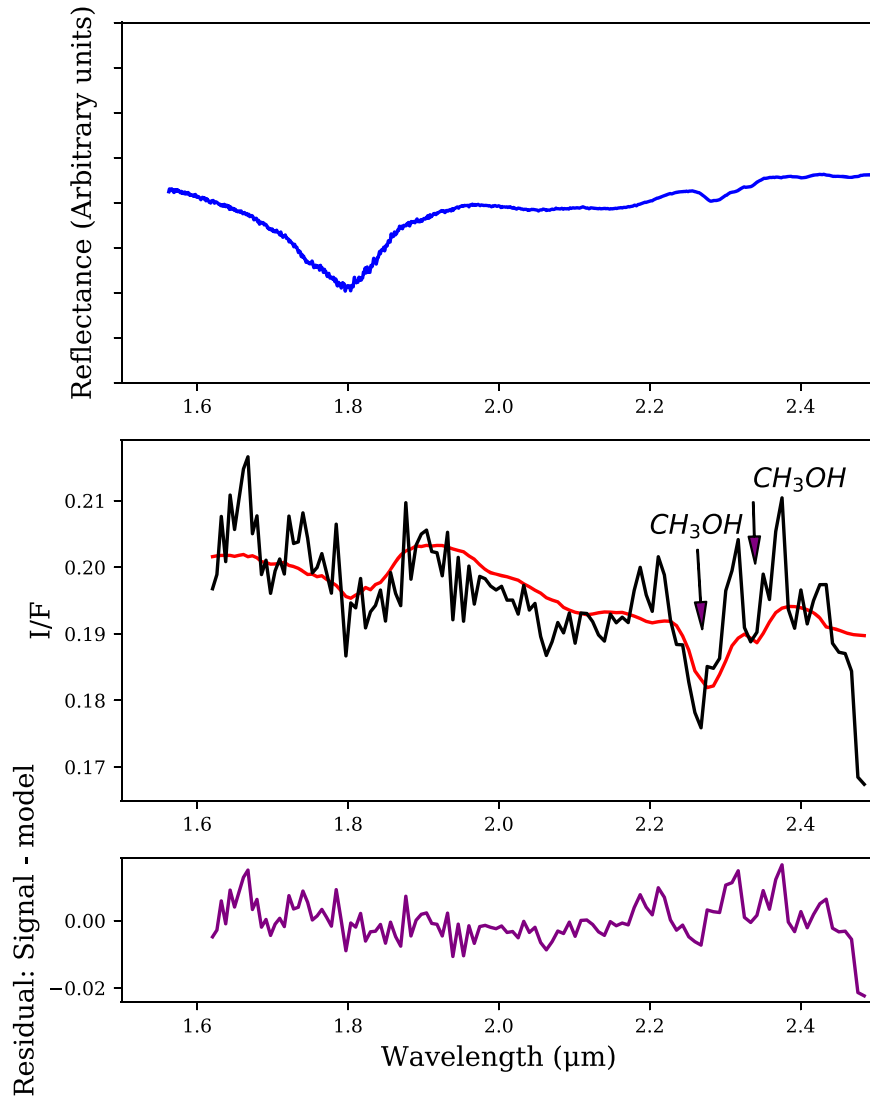


**Figure 2.** Comparison between the NIR spectrum of (486958) Arrokoth and laboratory sulfur-containing (CNOHS) tholins at  $1.8 \mu\text{m}$ . Top panel: spectrum of the “with sulfur” residue (scaled to Arrokoth reflectance). Middle panel: averaged NIR spectrum of (486958) Arrokoth (data from Stern et al. 2019), as measured by LESIA spectrograph aboard New Horizons spacecraft (black line) compared to linear mixture model of methanol + “with sulfur” residue + “without sulfur” residue (red line). Bottom panel: residual difference between Arrokoth spectrum and the model. Previously identified features at  $2.27$  and  $2.34 \mu\text{m}$  are attributed to methanol (Grundy et al. 2020). The linear model is obtained by fitting a linear combination of the spectra of the three compounds. This model could not be used for quantitative determination of relative abundances on the surface of Arrokoth. The model-fitting coefficients are:  $[0.6, 3.77, 1.46]$  for [methanol, “with sulfur,” “with sulfur”] and intercept =  $-0.94$ .

The strong bands at  $2.27$  and  $2.34 \mu\text{m}$  were previously assigned to methanol (Grundy et al. 2020). As discussed in Grundy et al. (2020) the  $1.8 \mu\text{m}$  feature could not be assigned to any of the simple molecular ices or organic tholins made of CNOH atoms. Methane, for example, would show additional bands around this region. Pure  $\text{H}_2\text{S}$  ice can also be excluded as origin of the  $1.8 \mu\text{m}$  feature because the absorption bands of  $\text{H}_2\text{S}$  are located at  $1.98$  and  $2.02 \mu\text{m}$  (Fathe et al. 2006) and no bands are observed at  $1.8 \mu\text{m}$  (Waggner et al. 1969). By screening spectra from USGS spectral library of most common minerals, we were able to rule them out. Indeed, while many minerals have a broad band between  $1.9$  and  $2.0 \mu\text{m}$ , none of them has the  $1.8 \mu\text{m}$  feature. The same arguments eliminate the orthorhombic sulfur,  $\text{S}_8$ . Thus, we propose that a sulfur-rich residue, produced by irradiation of ice containing  $\text{H}_2\text{S}$ , is the source of the  $1.8 \mu\text{m}$  feature. This scenario is rather plausible as the CC-KBOs are believed to have formed and resided beyond

$30 \text{ au}$ , where  $\text{H}_2\text{S}$  is stable for the time needed for the formation of organic crust of heteropolymers (Wong & Brown 2016).

The organic layer that is formed as a result of surface processing on small icy bodies, including KBOs, by photons and energetic particles is believed to be responsible for the spectral reddening observed in many of these bodies, including Arrokoth. The spectral slope in the NIR and visible spectral regions is a function of the chemical composition of the initial ices at the surface. As a consequence, spectrally intriguing characteristics of small bodies, such as the color bimodality observed in KBOs, Jupiter Trojans, and Centaurs, could be linked to the initial composition and irradiation history of these objects. To push this idea to more testable hypothesis, Wong & Brown (2016) demonstrated that the sublimation line of  $\text{H}_2\text{S}$  is located within the belt of primordial planetesimals. Therefore, these objects would have been divided into two groups: those that retained  $\text{H}_2\text{S}$  for enough time to develop a sulfur-containing organic crust, and those that did not. Laboratory

irradiation of ices with and without H<sub>2</sub>S supported the different NIR spectral reddening after irradiation with high fluence of electron irradiation: reddening slope is more pronounced in samples containing H<sub>2</sub>S (Poston et al. 2018) and these samples have the 1.8  $\mu$ m feature observed on Arrokoth. Further rigorous comparison to telescopic and spacecraft spectra will need laboratory measurements of optical constants for ice tholins with and without sulfur, requiring additional experimental work.



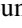
A broader implication of the organosulfur residue is the role it could play as a reservoir for sulfur in molecular clouds. The abundance of sulfur in dense clouds and circumstellar regions is only 0.1% of its cosmic abundance (Tieftrunk et al. 1994). Recent chemical models attempted to include sulfur residue in the modeling of the hot molecular cores (Woods et al. 2015), but a lack of accurate measurements of production rates of the residues hindered accurate evaluation of its role as sink for sulfur. Sulfur-rich residues have been proposed as an explanation for the sulfur depletion problem. The fact that sulfur tholins are not volatile means that they cannot be detected using ground-based submillimeter telescopic observations. The low dissociation energy of H<sub>2</sub>S (S–H bond energy = 363 kJ mol<sup>-1</sup>) and high reactivity of S atom and HS radical suggest a rapid conversion of H<sub>2</sub>S by irradiation chemistry. Garozzo et al. (2010) have demonstrated that H<sub>2</sub>S is almost completely consumed under the effect of ion irradiation at a dose of 21 eV/16 amu, producing multiple molecules, including a sulfur residue. While the authors in Garozzo et al. (2010) have not determined the production cross section of the residue, it is expected to be very high, because all the other sulfurous molecules explain only 30% of the consumed sulfur.

Thus, our finding of S-rich residue, likely sourced from H<sub>2</sub>S, has implications for both the present-day solar system and for pre-planetary systems. Arrokoth and all CC-KBOs are classified as ultra-red objects: color slope of 28% per 100 nm at 550 nm for Arrokoth (Grundy et al. 2020). Connecting the color slope of small icy objects in the solar system to a particular chemical composition could provide a very powerful way to trace back the history of the solar system and explicitly test results suggested by dynamical models (Morbidelli et al. 2005; Nesvorný et al. 2020). The chemistry and spectroscopy of S-rich residue could be a tracer for specific regions and specific environments of the early solar system (Wakelam et al. 2011).

This work has been supported by the NASA/RDAP program and by the Keck Institute for Space Studies (KISS).

This work has been conducted at the JPL, Caltech, under a contract with the National Aeronautics and Space Administration (NASA) and at the Caltech Division of Geological and Planetary Sciences.

### ORCID iDs

Ahmed Mahjoub  <https://orcid.org/0000-0003-1229-5208>  
 Michael E. Brown  <https://orcid.org/0000-0002-8255-0545>  
 Michael J. Poston  <https://orcid.org/0000-0001-5113-1017>  
 Bethany L. Ehlmann  <https://orcid.org/0000-0002-2745-3240>  
 Mathieu Choukroun  <https://orcid.org/0000-0001-7447-9139>  
 Kevin P. Hand  <https://orcid.org/0000-0002-3225-9426>

### References

- Bennett, C. J., Pirim, C., & Orlando, T. M. 2013, *ChRv*, **113**, 9086  
 Cartwright, R. J., Nordheim, T. A., Cruikshank, D. P., et al. 2020, *ApJL*, **902**, L38  
 Cruikshank, D. P., Imanaka, H., & Dalle Ore, C. M. 2005, *AdSpR*, **36**, 178  
 Fathe, K., Holt, J. S., Oxley, S. P., & Pursell, C. J. 2006, *JPCA*, **110**, 10793  
 Garozzo, M., Fulvio, D., Kanuchova, Z., Palumbo, M. E., & Strazzulla, G. 2010, *A&A*, **509**, A67  
 Grundy, W. M., Bird, M. K., Britt, D. T., et al. 2020, *Sci*, **367**, eaay3705  
 Hand, K. P., & Carlson, R. W. 2011, *Icar*, **215**, 226  
 Mahjoub, A., & Hodyss, R. 2018, *ApJ*, **869**, 98  
 Mahjoub, A., Poston, M. J., Blacksberg, J., et al. 2017, *ApJ*, **846**, 148  
 Mahjoub, A., Poston, M. J., Hand, K. P., et al. 2016, *ApJ*, **820**, 141  
 Materese, C. K., Cruikshank, D. P., Sandford, S. A., Imanaka, H., & Nuevo, M. 2015, *ApJ*, **812**, 150  
 Morbidelli, A., Levison, H. F., Tsiganis, K., & Gomes, R. 2005, *Natur*, **435**, 462  
 Nesvorný, D., Vokrouhlický, D., Alexandersen, M., et al. 2020, *AJ*, **160**, 46  
 Poston, M. J., Mahjoub, A., Ehlmann, B. L., et al. 2018, *ApJ*, **856**, 124  
 Rubin, M., Altwegg, K., Balsiger, H., et al. 2019, *MNRAS*, **489**, 594  
 Stern, S. A., Weaver, H. A., Spencer, J. R., et al. 2019, *Sci*, **364**, eaaw9771  
 Tieftrunk, A., Pineau des Forets, G., Schilke, P., & Walmsley, C. M. 1994, *A&A*, **289**, 579  
 Waggner, W. C., Weinberger, A. J., & Stoughton, R. W. 1969, *JPhCh*, **73**, 3518  
 Wakelam, V., Hersant, F., & Herpin, F. 2011, *A&A*, **529**, A112  
 Wong, I., & Brown, M. E. 2016, *AJ*, **152**, 90  
 Wong, I., Brown, M. E., Blacksberg, J., Ehlmann, B. L., & Mahjoub, A. 2019, *AJ*, **157**, 161  
 Woods, P. M., Occhiogrosso, A., Viti, S., et al. 2015, *MNRAS*, **450**, 1256